

High-Speed Radiographic Analysis of Subcutaneous Injection Depots: Dispersion, Morphology, and Diffusion in Autoinjector Delivery

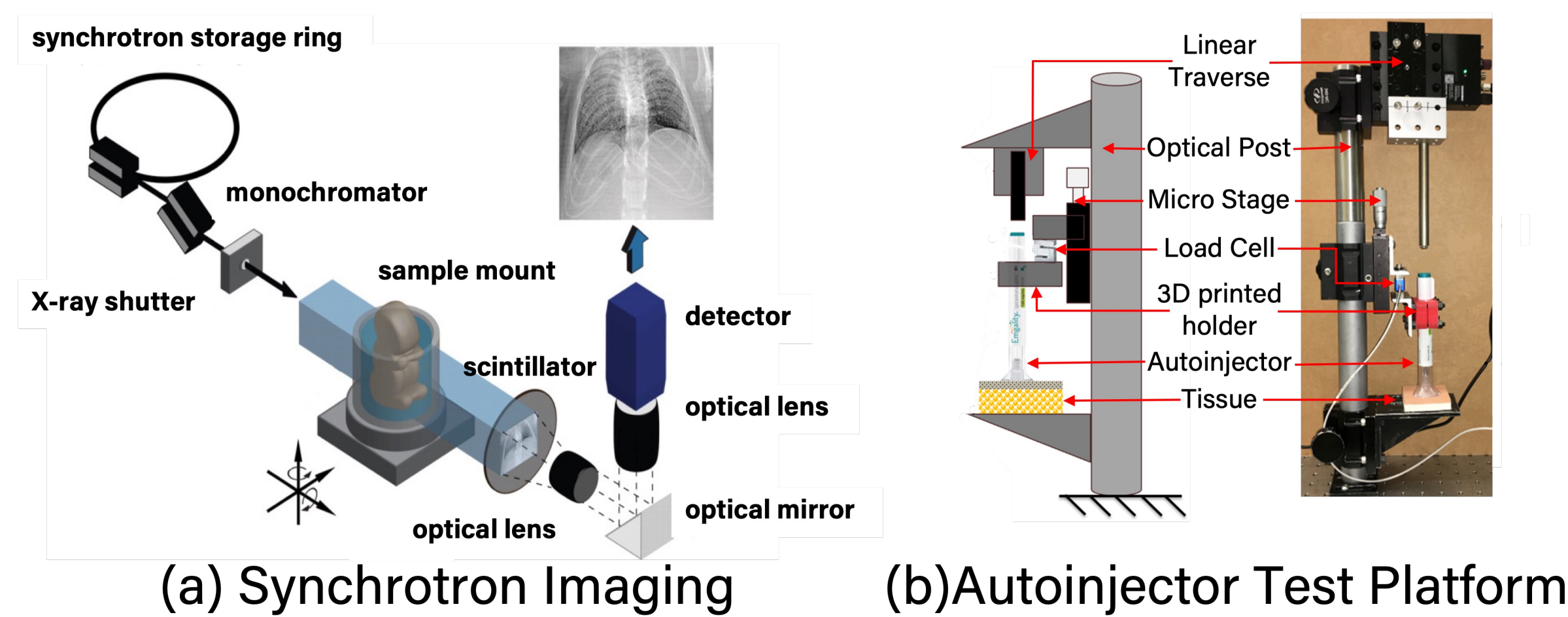
1. Introduction

❖ **Objective:** Experimentally investigate how autoinjector design parameters affect drug dispersion, depot morphology, and diffusion dynamics in subcutaneous (SC) tissue

❖ **Methodology:**

- Evaluated three autoinjector models designed to deliver 0.5, 1, and 2 mL. For this study, the autoinjectors delivered iodine solution ($\rho=1.34 \text{ gr/cm}^3$, $\mu=9.9 \text{ mPas}$) into excised pork belly tissue.
- Used high-speed synchrotron radiography for real-time 2D visualization of plume dynamics during injection.
- Used Synchrotron CT to capture the 3D morphology of the depot post-injection.

2. Methodology



Device	Number of samples	Volume [ml]	Needle Diameter	Needle Length [mm]	Spring Stiffness [N/mm]
Autoinjector1	9	0.5	29 G	12.7	0.22 ± 10%
Autoinjector2	9	1.0	27 G	12.7	0.20 ± 10%
Autoinjector3	9	2.0	27 G	8	0.26 ± 10%

- 2D and 3D plume images were segmented to calculate morphological parameters like volume, surface area, aspect ratio, and sphericity.
- Post-injection diffusion coefficients were derived using image analysis and real-time intensity distribution, following Ahmadzadegan et al. (2022).

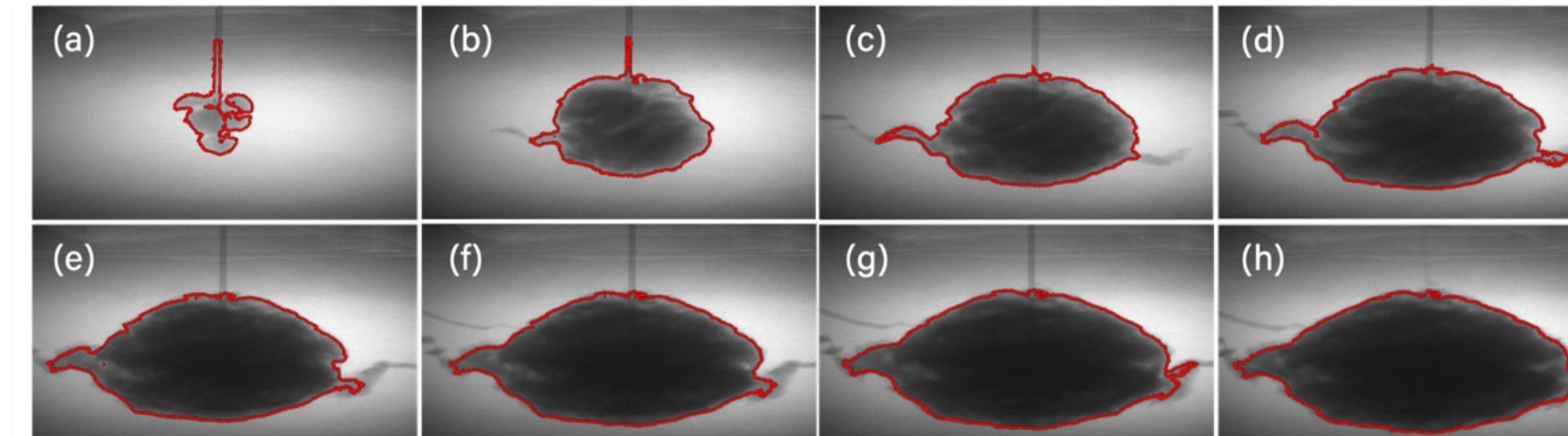
5. Conclusion

- Plume growth was non-linear, with a rapid initial phase followed by deceleration, and the final plume volume exceeded the delivered dose by 25% at the end of the injection due to product spread in the subcutaneous space.
- Plumes expanded primarily horizontally regardless of injection volume, with the horizontal-to-vertical aspect ratio increasing throughout the injection to a final value of ~4 across all devices.
- Tissue crack formation during injection significantly influenced plume morphology.

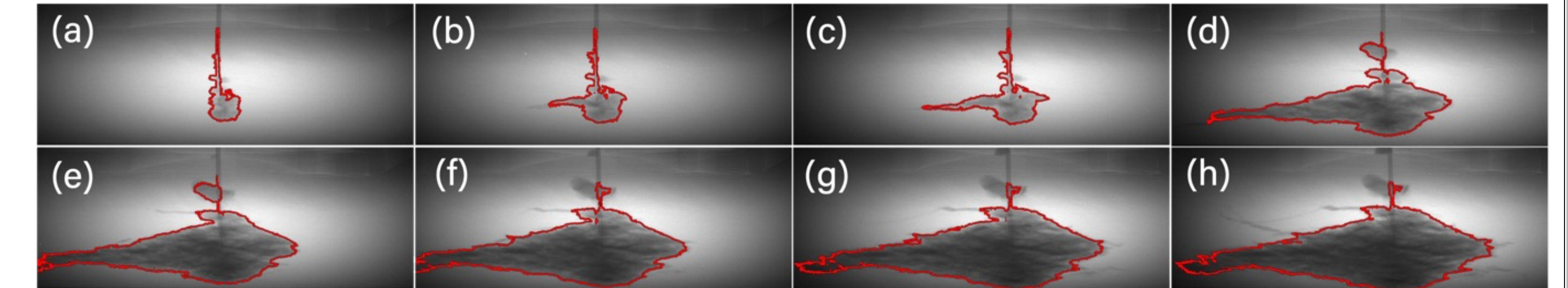
3. Plume Growth and Diffusion into the Tissue

❖ **Tissue Interaction**

Tissue crack formation during injection significantly influences plume morphology, spreading plume along crack pathways.



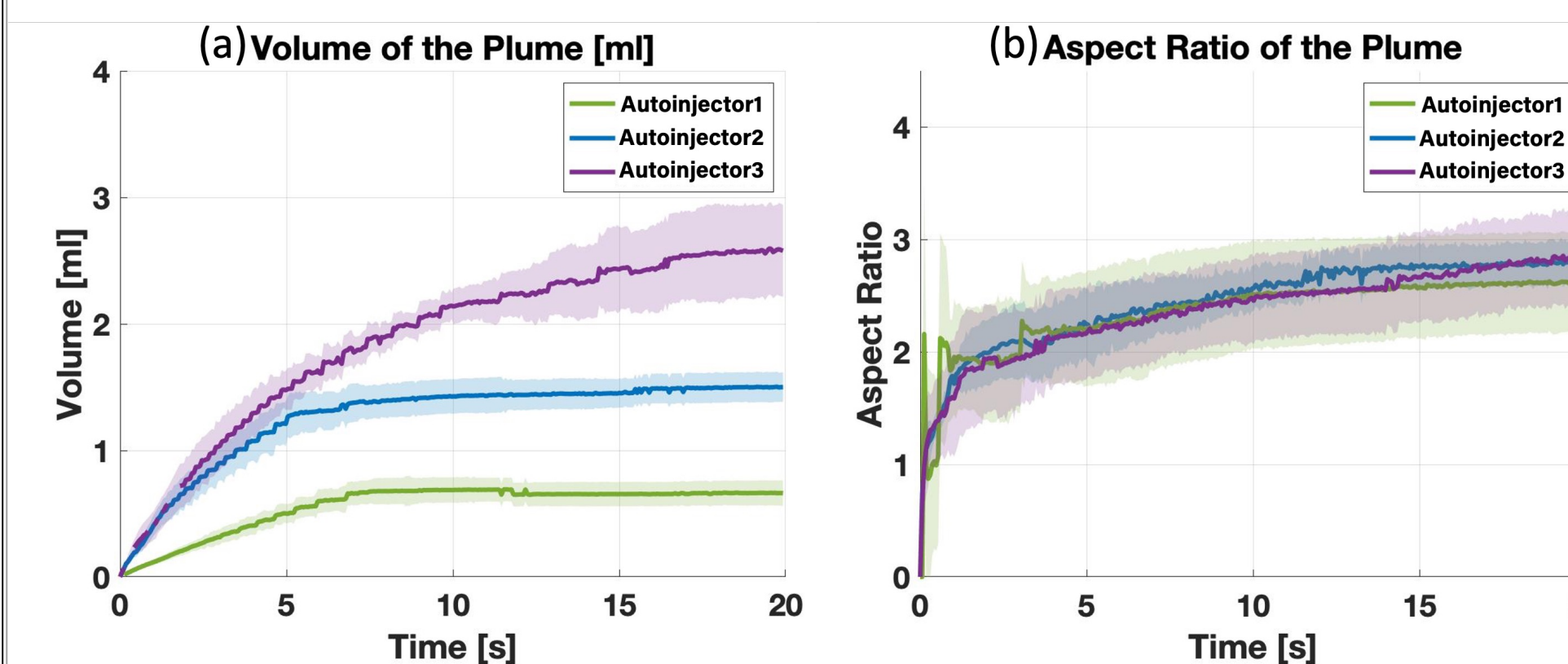
Segmented plumes from the start to the end of injection, including post-injection. The time interval between frames is 1.02 seconds.



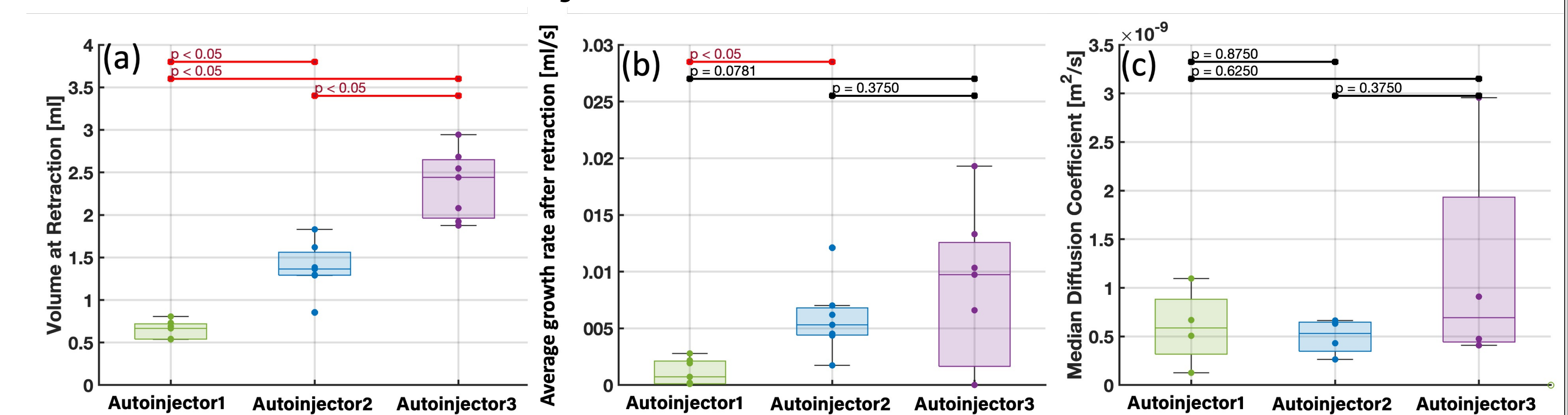
Time sequence of plume growth for case 7. The time interval between frames (a)-(c) is 0.06 seconds, and from (c)-(h) is 1.02 seconds. Frames (a)-(c) show crack formation on left side and accordingly drug spread in that direction

❖ **Plume Dispersion During and after Injection**

- Plume volume grows non-linearly, expanding rapidly at first due to maximum compression of the drive spring, then slowing as the spring decompresses.
- Aspect ratio > 1 throughout, increasing over time, confirming lateral plume growth dominates over vertical diffusion.



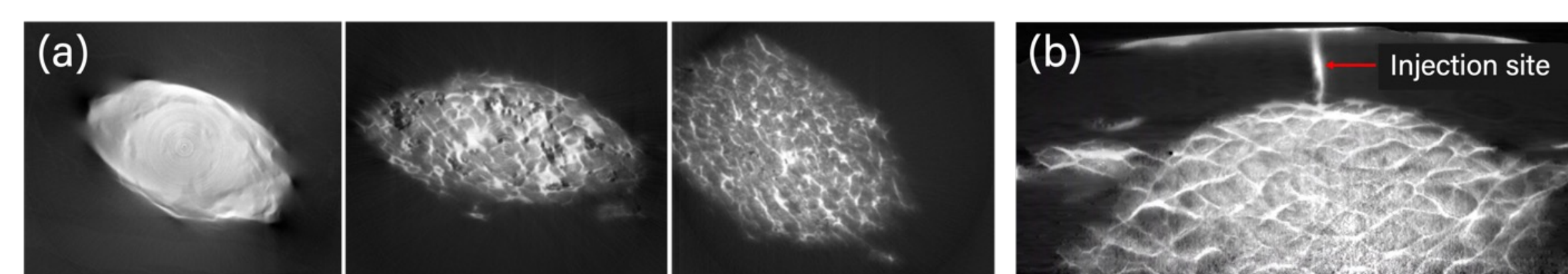
❖ **Plume Diffusion Post-Injection**



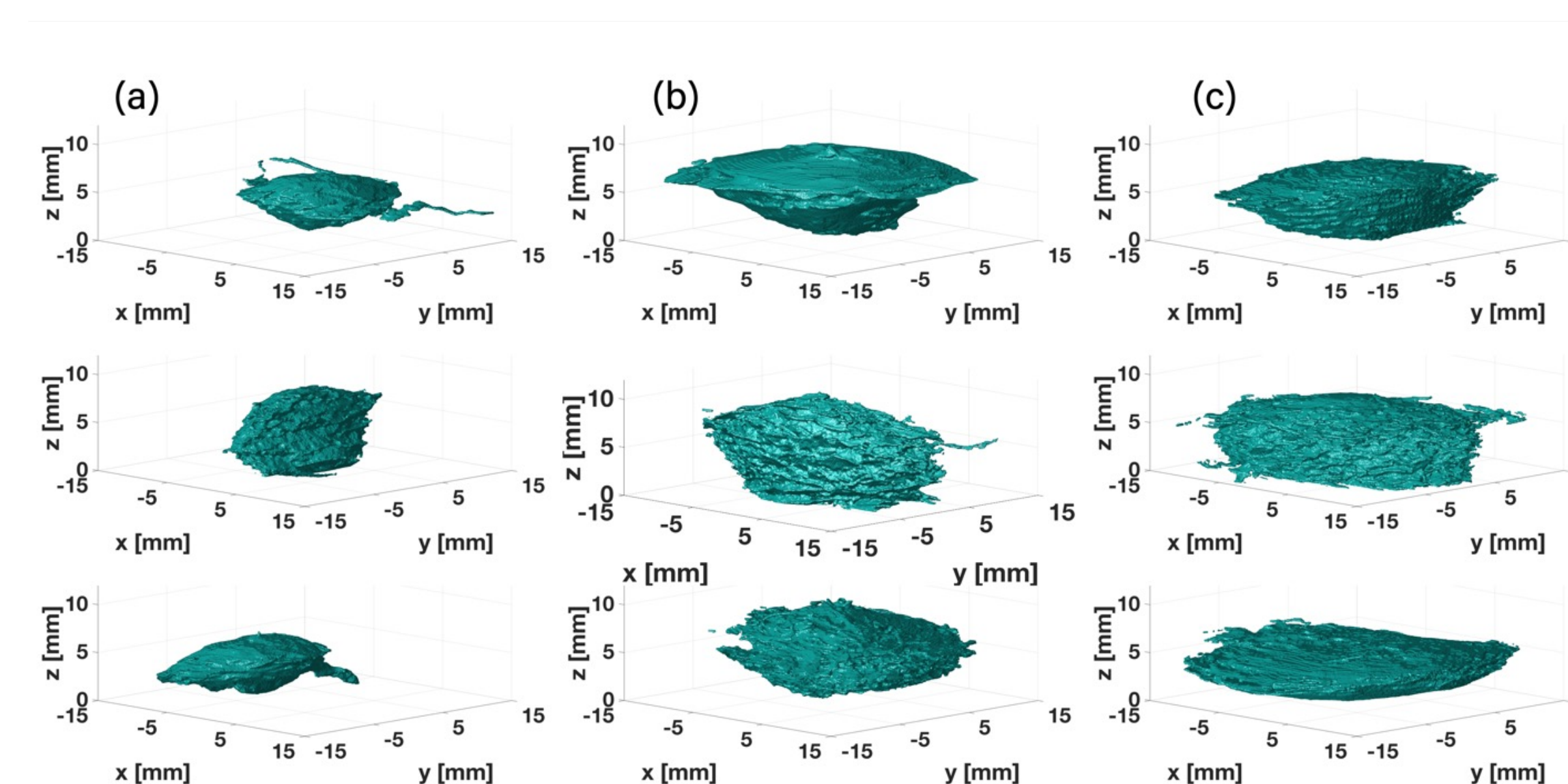
- Plot (a) shows calculated volumes exceeding nominal delivered volumes due to drug spread in tissue.
- Early post-injection growth rate and diffusion coefficient analysis show no significant differences between autoinjector models.
- Findings suggest diffusion is driven by tissue properties rather than device design or interstitial pressure variations.

4. 3D Plume Morphology

❖ **3D Plume Dispersion Post-Injection**



Synchrotron Computed Tomography (CT) Projections of Injected Plumes. (a) Top-down views of injected plumes using Autoinjector1, 2, and 3, respectively (from left to right). (b) A side view of the injected plume using Autoinjector2.



3D Plume Segmentation from CT Scans (a) 0.5 mL injection, (b) 1 mL injection, and (c) 2 mL injection using autoinjectors.

❖ **Statistical Analysis of 3D Plume Post-Injection**

- Plume surface area expands with increasing delivered drug volume.
- Sphericity inversely correlates with surface area, reflecting plume compactness.
- Post-injection, aspect ratios continue to rise, showing consistent distributions with no significant differences between autoinjector models.

